Research paper

Aluminum-air battery with cotton substrate: Controlling the discharge capacity by electrolyte pre-deposition

Wending Pan, Yifei Wang*, Holly Y.H. Kwok, Dennis Y.C. Leung**

Department of Mechanical Engineering, The University of Hong Kong, Hong Kong, China

Abstract

Conventional Al-air battery has many disadvantages for miniwatt applications, such as the complex water management, bulky electrolyte storage and potential leakage hazard. Moreover, the self-corrosion of Al anode continues even when the electrolyte flow is stopped, leading to great Al waste. To tackle these issues, an innovative cotton-based aluminum-air battery is developed in this study. Instead of flowing alkaline solution, cotton substrate pre-deposited with solid alkaline is used, together with a small water reservoir to continuously wet the cotton and dissolve the alkaline in-situ. In this manner, the battery can be mechanically recharged by replacing the cotton substrate and refilling the water reservoir, while the thick aluminum anode can be reused for tens of times until complete consumption. The cotton substrate shows excellent ability for the storage and transportation of alkaline electrolyte, leading to a high peak power density of 73 mW cm^{-2} and a high specific energy of 930 mW h g^{-1}. Moreover, the battery discharge capacity is found to be linear to the loading of pre-deposited alkaline, so that it can be precisely controlled according to the mission profile to avoid Al waste. Finally, a two-cell battery pack with common water reservoir is developed, which can provide a voltage of 2.7 V and a power output of 223.8 mW. With further scaling-up and stacking, this cotton-based Al-air battery system with low cost and high energy density is very promising for recharging miniwatt electronics in the outdoor environment.

© 2021, Institute of Process Engineering, Chinese Academy of Sciences. Publishing services by Elsevier B.V. on behalf of KeAi Communications Co., Ltd. This is an open access article under the CC BY-NC-ND license (http://creativecommons.org/licenses/by-nc-nd/4.0/).

Keywords: Al-air battery; Cotton-based; Electrolyte pre-deposition; Capacity control; Miniwatt electronics

1. Introduction

Nowadays, miniwatt electronic devices are employed ubiquitously in the model society, ranging from conventional 3C products to the upcoming wearable electronics. Restricted by the limited battery capacity, a frequent recharge is generally required, which is either accomplished indoor by electric grid or outdoor by various power banks. To date, the Li-ion battery based power bank is the most mature product in the market, but the energy density is not that satisfactory. Also, the power bank itself requires long time to recharge. To solve this issue, novel power sources have been developed for miniwatt applications, such as fuel cell and metal-air battery. These two devices are quite similar with each other expect for the type of fuel employed. In general, fuel cell uses gaseous and liquid fuels such as hydrogen, methanol and ethanol [1], while metal-air battery uses solid metal fuels such as aluminum, zinc and magnesium [2]. As for the oxidant, oxygen from ambient air is preferred in both devices. In this manner, fuel cell and metal-air battery can achieve much higher energy density than Li-ion battery, and the fuel can be instantly replenished for continuous operation.

Compared with fuel cell that requires expensive catalyst and membrane electrolyte, the metal-air battery is much more cost-effective. In addition, the solid form of fuel in metal-air battery eliminates the fuel crossover problem. Furthermore, metal-air battery generally provides higher voltage than fuel

* Corresponding author.
** Corresponding author.
E-mail addresses: wang1fei@connect.hku.hk (Y. Wang), ycleung@hku.hk (D.Y.C. Leung).
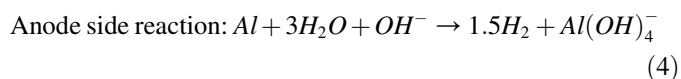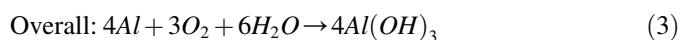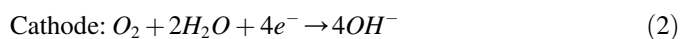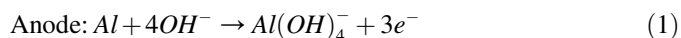
cell, which is mainly because of the lower oxidation potential of metals than other fuels. All these advantages make metal-air battery a step closer to the real market. In literature, various metal-air batteries have been proposed, such as Li-air [3], Zn-air [4], Al-air [5] and Mg-air battery [6]. Among them, the primary Al-air battery is especially promising for non-rechargeable missions. As shown in Table 1, Al has many advantages such as low reaction potential, high theoretical specific capacity and low price compared with Zn and Li [7–9].

Al-air battery was first proposed in 1962 by Zaromb et al. [10], which includes an aluminum anode, an air-breathing cathode and an electrolyte solution in between. Although it is a primary battery that cannot be recharged electrically, the Al-air battery can be mechanically recharged by replacing the exhausted Al anode, while the air-breathing cathode can be reused for a long time. As for the electrolyte, strong alkaline is commonly employed, such as sodium hydroxide (NaOH) and potassium hydroxide (KOH). The electrode reactions are described by the following equations. It is noticed that the OH^- is consumed on the anode side (Eq. (1)) and regenerated on the cathode side (Eq. (2)), so that the overall OH^- amount should not vary theoretically (Eq. (3)). In practical, however, the Al anode also has a side reaction, that is, the notorious Al self-corrosion which will consume OH^- (Eq. (4)). As for the water, it is consumed by both oxygen reduction (Eq. (2)) and Al corrosion (Eq. (4)). In this manner, the alkaline solution needs to be continuously supplied, which is generally accomplished by electrolyte circulation in conventional Al-air batteries.

Anode: $Al + 4OH^- \rightarrow Al(OH)_4^- + 3e^-$ (1)

Cathode: $O_2 + 2H_2O + 4e^- \rightarrow 4OH^-$ (2)

Overall: $4Al + 3O_2 + 6H_2O \rightarrow 4Al(OH)_3$ (3)

Anode side reaction: $Al + 3H_2O + OH^- \rightarrow 1.5H_2 + Al(OH)_4^-$ (4)

Till now, great efforts have been made to improve the performance of Al-air battery [11], including the study of Al alloy for the anode [12–14], oxygen reduction catalyst for the air cathode [15–17], and corrosion inhibitor for the electrolyte [18–20]. Based on these efforts, large Al-air battery systems with significant power output have been developed, which are mostly applied in stationary and transportation sectors such as uninterrupted power supply and electric vehicle [21]. As for miniwatt application, the conventional Al-air battery system is not only heavyweight but also complicated due to the bulky electrolyte storage and complex water management, not to mention the potential hazard of corrosive electrolyte leakage. To solve these problems, solid-state gel electrolytes have been developed for Al-air batteries in recent years. Although a relatively high discharge performance can be obtained by cost-effective and eco-friendly gel electrolyte [22], the power density is generally limited due to the impeded ion trans-portation inside [23–26]. Also, the discharge products cannot be effectively removed from the anode surface. Alternatively, paper-based Al-air batteries have been developed recently by using cellulose paper as electrolyte channel [27–29]. In this manner, only a limited amount of electrolyte is needed, which can be transported automatically by capillary action. More-over, the paper-based Al-air battery was found to possess other advantages such as corrosion inhibition [30], battery flexibility [31] and printable manufacture [32], which is especially suitable for low-power electronics such as lateral flow tests and biosensors. Nevertheless, due to the limited electrolyte storage of paper, the battery power output was quite low, and the discharge capacity at high current densities was not satisfactory, which is not suitable for recharging miniwatt electronics such as cell phones.

To improve the power output and discharge capacity, in this work, we have developed a cotton-based Al-air battery using low-cost industrial-grade Al plate as anode. Cotton was selected as substrate because of its higher electrolyte storage capability and lower diffusion resistance to the ions inside. In addition, a specific amount of solid alkaline was pre-deposited inside the cotton to both control the battery discharge capacity and enhance user safety, and a passive water reservoir was employed to keep the necessary wettability. Compared with other paper-based batteries and fuel cells in literature, our cotton-based Al-air battery achieved much higher power density and specific energy. In addition, the discharge capacity can be precisely controlled by the amount of pre-deposited alkaline, eliminating unnecessary Al waste due to self-corro-sion. Moreover, the battery was reusable if sufficient Al anode was stored inside, which could be mechanical recharged by replacing the cotton substrate and refilling the water reservoir.

2. Experimental

2.1. Battery materials

2.1.1. Al anode

Four types of Al, that is, pure Al with a purity of 99.999% or 99.99%, Al alloy 1060 with a purity of 99.6%, and kitchen foil Al with a purity of 97.5% were used in this study. The Al plate was cut into a rectangular shape with an effective reac-tion area of 1.5 cm × 1.5 cm. The Al surface was polished by silicon carbide paper, degreased in pure ethanol and air dried before assembling into the battery.

2.1.2. Air-breathing cathode

Carbon paper (HCP135, Hesen) was employed as gas diffusion layer, which was used to support the amorphous

Table 1
Comparison of reaction potential, theoretical specific capacity and price of aluminum, lithium and zinc metals.

Metal	Reaction potential vs SHE	Theoretical specific capacity	Price USD/Ton
Aluminum	−1.66 V	2, 980 mA h g^{-1}	1, 885
Zinc	−0.76 V	820 mA h g^{-1}	2, 573
Lithium	−3.04 V	3, 860 mA h g^{-1}	16, 500

MnO_2 catalyst. The catalyst ink was prepared by dispersing MnO_2 powder (AR, Qiangshun Chemical) in an ethanol-water solution (1:1) with 1 wt.% Nafion binder (Sigma-Aldrich). Next, the ink was sonicated for 1 h, which was finally dropped onto the carbon paper (1.5 cm × 1.5 cm) with an overall MnO_2 loading of 4 mg cm^{-2}.

2.1.3. Electrolyte substrate

Both filter paper (Grade 4, Whatman) and cotton (commercial makeup cotton) were tested in this work without further processing. In addition, the polyvinyl alcohol (PVA) film and peroxyacetyl nitrate (PAN) film were also tested for comparison purpose. The Brunauer-Emmet-Teller (BET) surface areas, Barrett-Joyner-Halenda (BJH) pore size distributions and pore volume of cotton substrate were measured through a N_2 adsorption analysis at 77 K using a Micromeritics ASAP 2020 analyzer. Detailed fabrication process of the PVA and PAN films can be found in the Supplemental Material.

2.2. Preparation of the alkaline cotton

To achieve high operation safety and quantitative battery discharge, solid-form alkaline cotton was employed as electrolyte, whose preparation process is shown in Fig. 1. First of all, an 8M NaOH solution was prepared by using NaOH pellets (Aladdin) and 18.2 MΩ deionized water (Barnstead). Next, a fixed volume of the NaOH solution was dropped onto the cotton substrate (1.5 cm × 1.5 cm), which was then dried on a hotplate at 185 °C. After complete drying, the as-prepared alkaline cotton was stored in a sealed tube to avoid NaOH deliquescing due to the water vapor in ambient air. The same operation was also repeated for the filter paper and PAN film, while the PVA film was directly immersed in the 8M NaOH solution and dried in order to obtain an alkaline polymer membrane. To study the effect of NaOH loading, a series of alkaline cottons containing different amounts of NaOH were prepared.

Morphology of the as-prepared alkaline cotton and other materials were examined by field emission scanning electron microscopy (FESEM, Hitachi S-4800FEG) while the elemental composition was investigated by energy dispersive x-ray analysis (EDAX).

2.3. Battery design and fabrication

A novel cotton-based Al-air battery was designed as shown in Fig. 2, which consisted of two main parts, i.e. the main block containing the water reservoir and the air-breathing cathode, and the drawer containing the Al plate and the alkaline cotton. They were fabricated by 3D printing using acrylonitrile butadiene styrene. For the main block, a water reservoir was located on the left side to store 0.25 mL (maximum) deionized water injected from the valve. On the right side, a cavity was left for inserting the drawer, while an air-breathing cathode was attached on its top and exposed to the ambient air. As for the drawer, a thick Al plate was stored on the bottom while the alkaline cotton was placed on its top. To operate the battery, the drawer was inserted into the main block, triggering the water uptake of alkaline cotton by capillary action and activating the battery in a few seconds. When the alkaline cotton was saturated with water, the battery performance reached its normal level and could be used to power other electronics until the alkaline was used up. During the discharge, water was continuously supplied from the reservoir to avoid cotton dry out, and the discharge capacity was well controlled by the amount of electrolyte inside the cotton. In this manner, no further corrosion of the Al plate occurred after the discharge mission, which is a strong advantage against conventional flow-based Al-air batteries. For the battery reuse, only the alkaline cotton needs to be replaced and the water reservoir to be refilled. The Al plate can also be refreshed once it is exhausted. With all lightweight materials, such a simplified battery system can achieve very high energy density compared with Li ion batteries, which is also more environmentally-friendly.

To improve its voltage and power output, a two-cell battery pack was also developed in this work, simply by separating the air cathode, Al plate and alkaline cotton into two parts and connecting the two cells in series by conductive tapes. A common water reservoir was employed to feed water to the single cells. To avoid the back diffusion of NaOH into the water reservoir, a buffer layer of blank cotton was added between the alkaline cotton and the water feeding hole. Battery packs with more single cells could be developed in the same way.

2.4. Electrochemical testing

After battery assembly, the open circuit voltage (OCV) was recorded first until it stabilized. Next, the polarization curve was obtained by Linear Sweep Voltammetry (LSV) from OCV to 0 V with a sweep rate of 25 mV s^{-1}. Afterwards, electrochemical impedance spectroscopy (EIS) test was conducted at
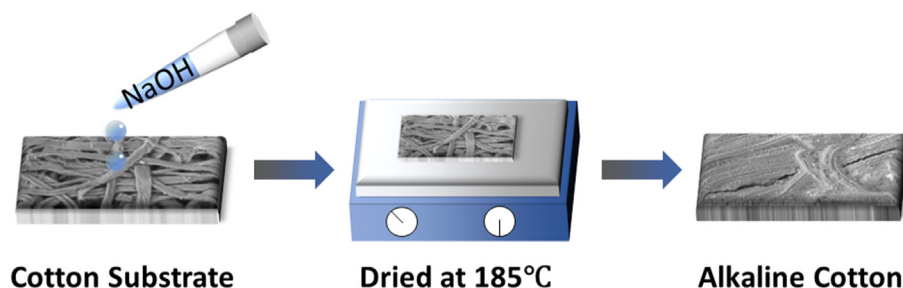

Fig. 1. Schematic diagram of the fabrication process of the solid alkaline cotton.
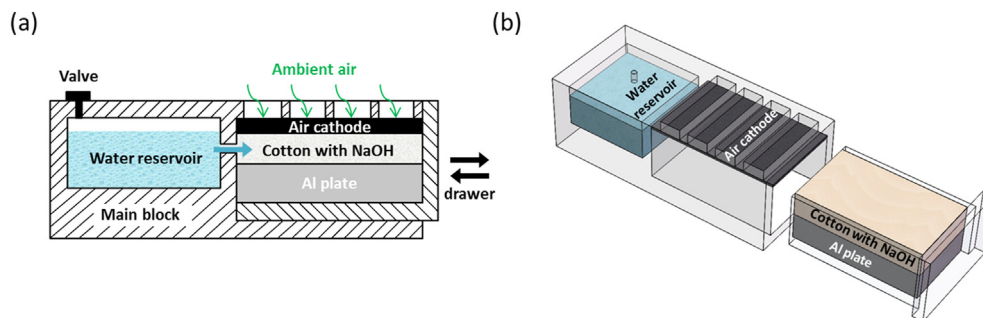
Fig. 2. Design and fabrication of the cotton-based Al-air battery: (a) Cross-sectional view; (b) 3D structure of the battery.

OCV from 1M Hz to 1 Hz, with an amplitude of 5 mV. To investigate the battery stability, Galvanostatic discharge was conducted at 10 mA cm^{-2} and the cutting voltage was set to zero. This current density was selected so that a scaled-up cell with 10 cm × 10 cm electrode can provide a current output of 1 A, which is sufficient for most miniwatt electronics. After battery discharge, the remaining Al plate was taken out and the corrosion products on its surface was removed. Its weight loss was used to calculate the specific capacity and specific energy. For comparison purpose, a control group was also tested by using untreated cotton substrate containing 0.25 mL of 8M NaOH solution (without water reservoir). All electrochemical tests were carried out using an electrochemical workstation (CHI660E) at room temperature (298 K).

3. Results and discussion

3.1. Effect of Al purity

Al purity was reported to significantly influence the Al-air battery performance especially the self-corrosion rate, which also determines the metal price [33]. In this section, the effect of Al purity was investigated first in our battery system. Four types of Al with representative purities were tested, including the 5N Al (99.999%), 4N Al (99.99%), the 2N6 Al alloy (99.6%) and the kitchen foil Al (97.5%). Their elemental compositions and market prices are compared in Table 2.

As shown in Fig. 3a, the 5N, 4N and 2N6 Al obtained similar performance with each other, which were all much higher than the kitchen foil Al. The obtained peak power densities were 30, 40 and 44 mW cm^{-2}, respectively, compared with 18 mW cm^{-2} for the kitchen foil Al. Although 5N Al obtained the highest OCV of 1.7 V, its power density was slightly lower than 4N and 2N6 Al anodes, which might be due to the more stable passive film on its surface. On the contrary, the 4N and 2N6 Al anodes with less purity could obtain more efficient removal of passive film due to the impurities, leading to larger reaction surface area and higher power output [34]. This was confirmed by the Nyquist plots in Fig. S2, where the battery with 5N Al anode shows the largest loop at high frequency range, reflecting the highest charge transfer resistance. Fig. 3b shows the continuous discharge test of 5N, 4N and 2N6 Al at 10 mA cm^{-2}. It was found that the 5N Al exhibited both a higher voltage plateau and a longer

discharge time than 4N and 2N6 Al. The specific capacity of 5N Al was also much higher than those of 4N and 2N6 Al, as shown in Fig. S3. This indicates that the higher purity Al is more favorable for high voltage discharge with better energy efficiency. In conclusion, the impurities inside Al anode may have positive effect on its passive film removal and peak power output, but will inevitably bring more significant corrosion, leading to less voltage output and energy efficiency. As for practical applications, the Al market price should also be considered. The energy output over cost is calculated to be 386, 78.5 and 1.3 Wh/USD for 2N6, 4N and 5N Al, respectively, so that the 2N6 Al is a much more cost-effective choice, which can compensate its slightly lower discharge performance. Therefore, 2N6 Al was selected as anode for subsequent studies.

3.2. Effect of electrolyte substrate

In addition to Al purity, the electrolyte substrate can also influence the battery performance due to the varied water uptake rate, pore size and porosity. In this section, different electrolyte substrates, that is, cotton, paper, PVA film and PAN film, were compared to select the best choice. Among them, the porous cotton, paper and PAN film were made of micro fibres that could store solid NaOH particles inside, so that pre-deposited electrolyte and water reservoir were adopted for battery operation; while the dense PVA film was directly immersed in 8M NaOH and dried in order to obtain an alkaline polymer electrolyte. This polymer electrolyte did not need water supply during battery operation, which was reported to exhibit excellent performance in fuel cells [35]. To make a fair comparison, the amount of pre-deposited NaOH (1 mmol) and water storage (0.125 mL) were controlled for the cotton, paper and PAN cases. In this manner, the final NaOH concentration was 8M, which was exactly the same with the PVA case.

Before the comparison, three different types of makeup cottons in the market were compared first as shown in Fig. 4a, which showed similar performance with each other. This result indicates that the quality of commercial makeup cottons is quite consistent, which does not influence the performance of our cotton-based Al-air battery. Fig. 4b indicates that the battery with cotton substrate achieved the highest maximum power density among all four substrates, while the PVA and PAN substrates exhibited limited power output. Compared

Table 2
Composition and market price of the three types of Al.

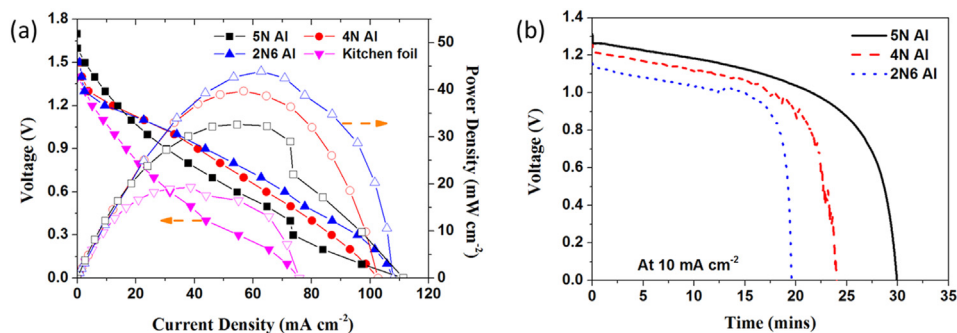| Type of Al	Al (%)	Fe (%)	Cu (%)	Mg (%)	Zn (%)	Mn (%)	Ti (%)	Si (%)	Other (%)	Price (USD/kg)
Kitchen foil	97.5	1.0	0.1	0.1	0.1	0.1	0.1	0.8	0.15	0.4
2N6	99.6	0.35	0.05	0.03	0.05	0.03	0.03	0.25	0.05	2.5
4N	99.99	No more than 0.01								13.5
5N	99.999	No more than 0.001								1200

Fig. 3. Performance comparison among different Al anodes using 0.5 mmol NaOH pre-stored in cotton: (a) Battery polarization curves; (b) Galvanostatic discharge test at 10 mA cm^{-2}.

with conventional Al-air batteries with direct aqueous electrolyte, which can generally reach hundreds of mW cm^{-2} [36–38], the power output of cotton-based Al-air battery is relatively lower (Table 3). This is mainly due to the fibre network inside the cotton substrate, which brings extra diffusion resistance and hence an increased ionic resistance. However, when compared with paper-based Al-air batteries with peak power density of only 20–30 mW cm^{-2} in literature, a substantial improvement is still obtained thanks to the higher porosity of cotton. As for the purpose of cotton substrate, it is mainly utilized to quantitatively control the discharge capacity as well as prevent any electrolyte leakage, which will be discussed in the following section. The battery impedance was examined by EIS test as shown in Fig. 4c, which could reveal the dynamic behaviour of redox reaction, double layer capacitance and mass diffusion. It was found that all four substrates had a similar polarization resistance as indicated by the same diameter of the semicircle. The cotton and paper substrates had relatively low ohmic resistance due to their high porosity for electrolyte transportation, while the PVA film had the highest ohmic resistance due to the lack of water content. As for the diffusion process, it was represented by the linear part of the EIS curve, which was fitted by Zview according to the Warburg impedance equation in below:

$$Z_w = \frac{A_w}{(iBw)^P} * \tanh((iBw)^P) \tag{5}$$

$$B = \frac{L^2}{D} \tag{6}$$

where "A$_W$" is the Warburg coefficient, "i" is the imaginary unit, "B" is the diffusion interpretation, "w" is the angular frequency, "P" is the exponential factor, "L" is the diffusion layer thickness and "D" is the diffusion coefficient. Table 4 summarizes the fitted parameters. All the P values were around 0.5, indicating that it was exactly the Warburg diffusion in our battery system. According to Eq. (6), the diffusion coefficient of OH$^-$ is in inverse proportion to the B value, so that the PAN film had the highest diffusion coefficient of OH$^-$ due to its smallest B value, indicating that PAN fibre is an excellent ion-conducting substrate. However, its maximum power density was poor because of its deficient water transportation ability, which greatly decreased the reaction rate at high current densities. This was proved by the water diffusion test as shown by the inset of Fig. 4c, in which the three porous substrates (cotton, paper and PAN) were placed in vertical with one end immersed in the methyl orange solution at the same time. The cotton achieved the fastest water diffusion while the PAN film obtained the slowest result. Considering the second smallest B value of cotton, it was concluded that the superior power output of cotton-based Al-air battery was benefited from its high diffusion ability of both water solvent and OH$^-$ ions.

To explain the difference in their water diffusion rate, microstructure of the different substrates with or without pre-deposited NaOH was compared in Fig. 4d. When NaOH was not deposited, the cotton and paper showed much more loose structure than the PAN film (insets), which was originated from their long and thick fibres that intertwined with each other. After NaOH deposition, the cotton substrate still exhibited a high porosity because of its high specific surface area of 19.11 m^2/g tested from BET analysis (Fig. S4), which is much higher than 1 m^2/g of filter paper [39,40]. On the contrary, the dense structure of paper and PAN film after NaOH deposition strongly prevented the diffusion of water. As for the PVA film, it had a compact surface with multiple cracks, which could be due to the vacuum drying process during SEM testing that reduced its original water content.
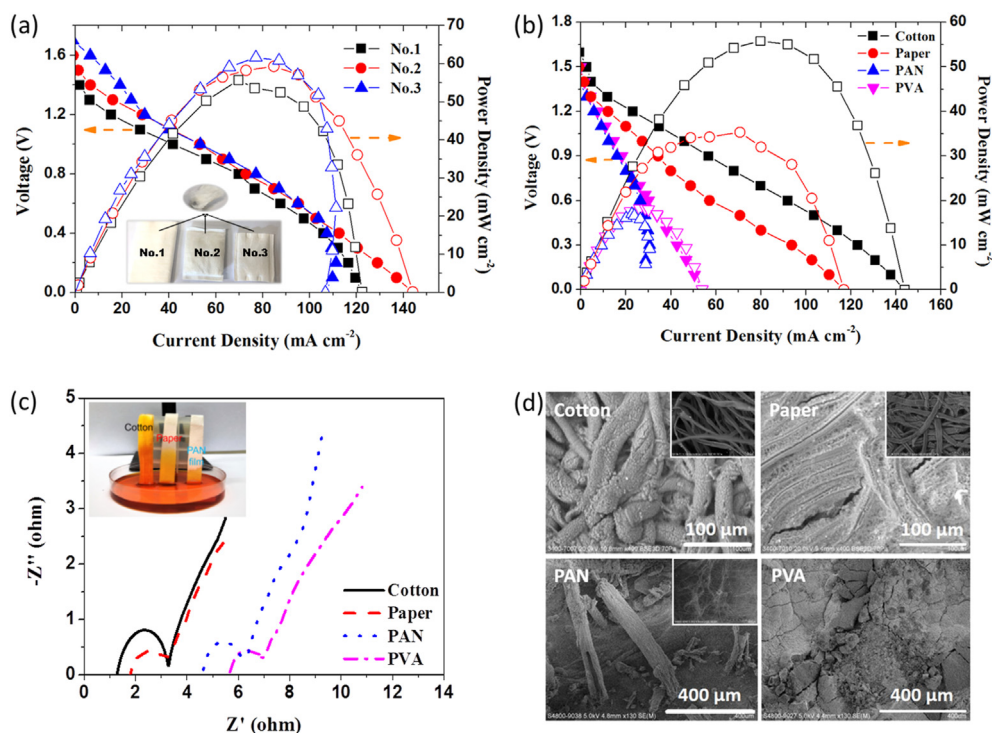
Fig. 4. Performance comparison among different types of electrolyte substrates: (a) Battery performance tested with different makeup cottons; (b) Battery performance tested with different substrates; (c) Nyquist Plot of the batteries with different substrates (inset: water diffusion test using methyl orange); (d) Surface morphology of the different substrates with pre-deposited NaOH (inset: the pristine substrates).

Table 3
Comparison of the Al-air battery performance with different types of electrolyte in recent literature.

Reference	Anode	Electrolyte	Cathode	OCV	Peak power density
Xue et al. [37]	4N Al	4M KOH	$(La_{1-x}Sr_x)_{0.98}MnO_3$	1.8V[a]	191.3 mW cm^{-2}
Li et al. [36]	Al plate	6M KOH	Co_3O_4/Co-N-C	1.7V[a]	160 mW cm^{-2a}
Xue et al. [15]	4N Al	4M KOH	$La_{0.7}(Sr_{0.15}Pd_{0.15})MnO_3$	1.9V[a]	265.6 mW cm^{-2}
Hopkins et al. [38]	5N Al	4M NaOH	Nano-Mn		300 mW cm^{-2}
Wang et al. [30]	1N Al	Paper-based	MnO2/C	1.6V	27.1 mW cm^{-2}
Shen et al. [28]	Al foil	Paper-based	Pd/C	1.55V	22.5 mW cm^{-2}
This work	2N6 Al	Paper-based	MnO_2	1.5V	35 mW cm^{-2}
This work	2N6 Al	Cotton-based	MnO_2	1.6V	55 mW cm^{-2}

[a] Estimated from figure.

Further test was conducted to compare the discharge stability between the cotton and paper substrates at 10 mA cm^{-2} with 3 mmol pre-deposited NaOH. Here, three layers of paper were used because a single layer of paper could only store about 1 mmol NaOH to the maximum. As shown in Fig. 5a, the cotton-based battery could be discharged for about 130 min until the NaOH was exhausted, which was 60% longer than the paper-based battery. Also, the average voltage of 1 V was 18% higher than the latter. As a consequence, a higher specific energy of 930 mW h g^{-1} was achieved by the cotton substrate. This superiority could be explained by the distribution of alkaline particles inside the substrate. As shown in Fig. 4d, compared with the loosely intertwined fibres of cotton that could absorb the alkaline particles uniformly from surface to inside, the densely-weaved fibres of paper accumulated the alkaline particles mainly on its surface. In this manner, excessive alkaline was provided to the electrode in the beginning and insufficient alkaline was supplied in the end, leading to severe Al corrosion at first and NaOH starvation later on for the paper-based Al-air battery. On the contrary, the cotton substrate was more uniform during the supply of alkaline electrolyte, which led to more stable discharge together with higher energy efficiency. This conclusion was further proved by the cross-sectional view of cotton substrate in Fig. 5b, where the NaOH particles were uniformly distributed among the fibres. Here, it is also worth mentioning that the cotton-based electrolyte delivery was found to inhibit the Al corrosion effectively during battery discharge. To prove this, a conventional Al-air battery with 2N6 Al as anode and MnO_2 as cathode was tested, using 8M NaOH solution directly as electrolyte. The battery was discharged at 10 mA cm^{-2} for 130 min (Fig. S5), and the calculated specific energy was only

Table 4
Parameter fitting from the linear part of EIS curves.

Substrates	$A_w(\Omega/s^{1/2})$/Error	B(s)/Error	P/Error
Cotton	4.08/4.2%	0.22/6.9%	0.53/1.6%
Paper	5.07/4.3%	0.36/7.9%	0.50/1.2%
PVA film	5.62/5.3%	0.25/9.6%	0.50/2.3%
PAN film	4.37/8.6%	0.11/13.2%	0.56/3.4%

348 mW h g^{-1} due to significant Al corrosion loss, which was much lower than that of the cotton-based cell (930 mW h g^{-1}).

3.3. Effect of the water supply

Compared with conventional Al-air batteries with flowing electrolyte, the cotton-based Al-air battery in this work relies on the cotton substrate for both electrolyte storage and water transport, which makes it pumpless and less prone to leakage issues. However, the cotton substrate can easily get dried during long-term operation due to both water evaporation and consumption. Therefore, passive water supply from a reservoir is necessary. Fig. 6a compares the battery discharge with and without the water reservoir, indicating that more stable discharge could be achieved with continuous water supply. As a result, the specific energy was significantly promoted. The poorer discharge performance of the latter case could be explained by the gradually increased ohmic resistance and impeded reaction kinetics due to the loss of water.

To better illustrate the significance of water supply, a mathematical model coupling the Millington Quirk correction, species transport equation and electric potential equation was further developed, which was solved by the commercial software Comsol. The computational domain and the key import parameters can be seen in Fig. S1 and Table S1, respectively. The governing equations are listed as follow:

$$D_i = \epsilon^{4/3} D_{i0} \tag{7}$$

$$\nabla \cdot (\rho U Y_i) - \nabla \cdot (\rho D_i \nabla Y_i) = S_i \tag{8}$$

$$S_i = \frac{\gamma_i \nabla i}{n_i F} \tag{9}$$

where ϵ is the porosity, ρ is the electrolyte density, U is the electrolyte velocity (zero in the current case), Y is the concentration of water or NaOH, D is the diffusion coefficient of water in cotton or NaOH in water, S is the production/consumption rate of water/NaOH due to electrochemical reactions. Only water and NaOH were studied in this simulation, while O$_2$ was regarded to be supplied sufficiently [41]. As shown in Fig. 6b, when there was no water reservoir, the NaOH concentration on the cathode side increased quickly because of the continuous NaOH generation and water consumption (Eq. (2)), which may cause serious side reactions. As for the anode side, the NaOH concentration slightly decreased, which was the compromise between NaOH and water consumption at the same time (Eq. (1) & Eq. (4)). On the other hand, when water reservoir was added, both the anode and cathode side encountered a decreasing NaOH concentration,

indicating that water was sufficiently provided during battery discharge. Nevertheless, the NaOH concentration was still more than enough to support a discharge current density of 10 mA cm^{-2} as indicated by Fig. 6a.

3.4. Effect of NaOH loading

For practical applications, when electricity is no longer needed, the conventional Al-air battery is very difficult to stop completely due to the remaining electrolyte inside channel that causes Al corrosion. Using water to rinse the channel is an effective solution, but will increase the system complexity as well as decreasing the energy density, which is not suitable for miniwatt applications. As for the present cotton-based Al-air battery, the battery discharge capacity can be precisely controlled by the loading of pre-deposited NaOH inside the cotton, eliminating the waste of Al anode.

In this section, different NaOH loadings were studied for the cotton-based Al-air battery. As shown in Fig. 7a, the battery performance was significantly improved when the NaOH loading increased. The peak power density elevated from 38.5 mW cm^{-2} with 0.5 mmol NaOH to 72.6 mW cm^{-2} with 4 mmol NaOH, which were all higher than batteries using 2−8M NaOH solutions dropped directly onto the cotton substrate (28−37.5 mW cm^{-2}, Fig. S6). According to Fig. 7b, a linear relation between the NaOH loading and the peak power density was confirmed (R^2 = 97.4%), indicating that the power output of the present battery could be precisely controlled. Moreover, Fig. 7c illustrates the effect of NaOH loading on the battery discharge lifetime, from which it was observed that a higher NaOH loading led to a longer discharge time due to the increased amount of reactant. The longest discharge time of 130 min was achieved by 3 mmol NaOH, while further increase of the NaOH loading to 4 mmol would lead to a reduction of discharge time. On the contrary, the battery with 8M NaOH electrolyte (0.25 mL solution dropped onto cotton substrate) could only discharge for 21 min (Fig. S7), which was 1/6 of the 3 mmol case. Fig. 7d presents the relationship between the NaOH loading (0.5−3 mmol) and the discharge time, which was also highly linear (R^2 = 99.2%). Based on this, the practical discharge lifetime (T) can be calculated by the following equations:

$$T = C * T_{theory} \tag{10}$$

$$T_{theory} = \frac{\frac{3}{4} NF}{J * S} \tag{11}$$

where "T$_{theory}$" is theoretical discharge lifetime (s), "N" is the NaOH loading (mol), "J" is the discharge current density (A m^{-2}), "S" is the electrode area (m^2), "F" is the Faraday constant (96,485 C mol^{-1}), and "C" is an empirical correction factor considering the corrosion loss (C = 0.75 according to Fig. 7d).

To further investigate the Al utilization efficiency, the discharge curves in Fig. 7c was transformed from "discharge time-voltage diagram" to "specific capacity-voltage diagram"
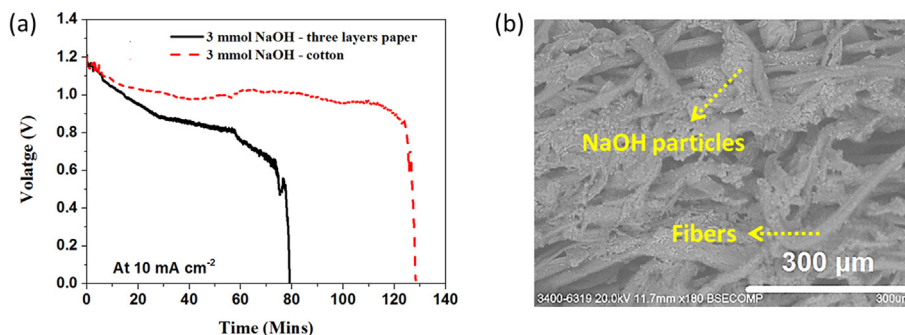
Fig. 5. Discharge comparison between the cotton and paper substrate with 3 mmol pre-deposited NaOH: (a) Galvanostatic discharge curve at 10 mA cm^{-2}; (b) SEM image of the cross-sectional view of the NaOH-deposited cotton.
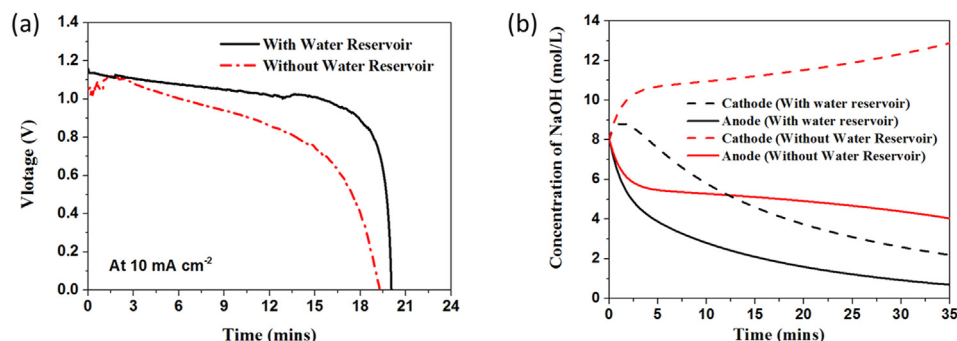

Fig. 6. (a) Discharge test at 10 mA cm^{-2} with and without water reservoir; (b) Variation of the NaOH concentration on the anode and cathode side during the discharge.

as shown in Fig. S8, using the weight loss of Al anode after each discharge test. Apparently, the discharge specific capacity with different NaOH loadings from 0.5 to 3 mmol all located around 1000 mA h g^{-1}, which had no discernible relationship with the NaOH loading. This is mainly because of the excess Al supply in the current battery design, so that the specific capacity is more related to Al properties, such as its purity. However, when the NaOH loading further increased to 4 mmol, a reduced specific capacity of 700 mA h g^{-1} was observed, indicating that higher NaOH loading can lead to severer Al corrosion. Therefore, 3 mmol should be the upper limit of NaOH loading for this cotton-based Al-air battery.

3.5. Battery stacking and application

A two-cell battery pack connected in series was developed in the end to improve the voltage and power output. As shown in Fig. 8a, the OCV was increased from 1.6 V to 2.7 V, while the peak power output was almost doubled from 112.5 mW to 223.8 mW. However, the maximum current was slightly lower than the single battery case, which could be due to the extra ohmic resistance from connection or the variation of single cell performances. With two more single cells stacked in series and an increased electrode area of 10 cm × 10 cm, a practical output of 5 V and 1 A can be projected, which is already sufficient for cell phone recharge. Fig. 8b illustrates the discharge stability of the two-cell battery pack. The discharge

plateau voltage was about 2.0 V, which was two times of the single cell voltage. Also, the discharge lifetime was almost the same with the single cell case, indicating a negligible internal self-discharge inside the stack. Furthermore, it was demonstrated for lighting up a number of LEDs as shown by the inset of Fig. 8b.

For the relatively short discharge time and unsatisfactory power in Fig. 8, it is mainly due to the lower NaOH loading of 1 mmol used for stack study. To improve them, a higher NaOH loading of 3 mmol is preferred as indicated by Fig. 7, which can further increase the battery performance and discharge lifetime. Furthermore, the scale of stack can be enlarged according to the mission profile, including the number of single cells and the electrode area of each cell, so that the stack voltage, power and lifetime can be further enhanced. As for the downward trend of working voltage in Fig. 8b, this is mainly due to the continuous consumption of OH$^-$ at the anode surface, which can only be supplemented from the regenerated OH$^-$ at cathode in our battery design. To improve the diffusion of OH$^-$ from cathode to anode, a thinner cotton substrate with higher porosity and lower tortuosity can be helpful, which might help to improve the discharge voltage stability.

Since 3 mmol is determined to be the upper limit of NaOH loading, to further improve the discharge lifetime, the cotton volume needs to be increased, which inevitably impairs the battery portability. Therefore, the current cotton-based Al-air battery system may be more suitable for short-term and
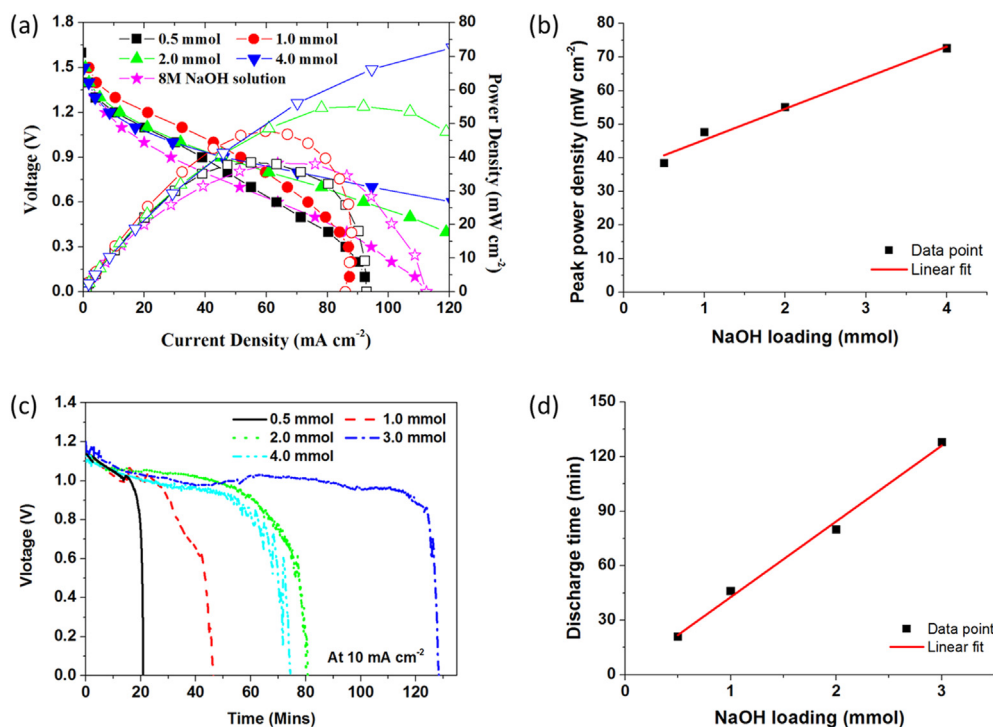
Fig. 7. Effect of NaOH loading on the cotton-based Al-air battery performance: (a) Comparison of the polarization curves; (b) Linear fitting of the peak power density; (c) Comparison of the Galvanostatic discharge curves at 10 mA cm^{-2}; (d) Linear fitting of the discharge lifetime.
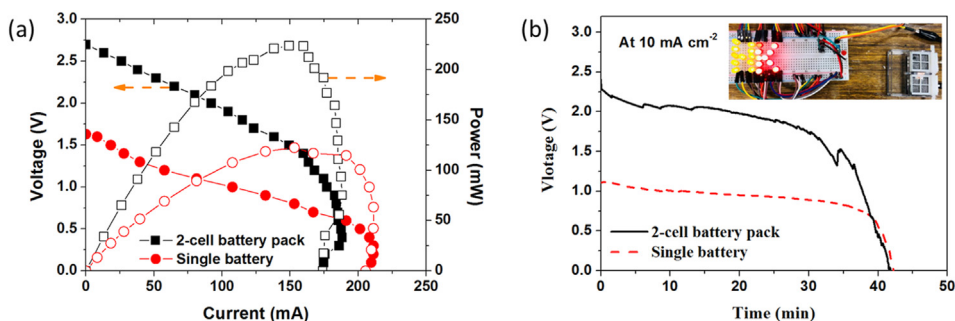

Fig. 8. Performance comparison between a single battery and a battery pack with two cells connected in series, both of which used 1 mmol NaOH in the cotton substrate: (a) Polarization curve; (b) Discharge test at 10 mA cm^{-2} (inset: LED lighting demonstration).

repetitive applications instead of long-term discharge missions, such as recharging of cell phone and mini drones. By replacing the exhausted cotton with a fresh one, our battery can work for multiple times without performance degradation, and the discharge lifetime can be precisely selected to avoid energy wastage.

4. Conclusion

In this work, a low-cost and high-energy-density Al-air battery with cotton substrate was successfully developed. By pre-storing solid alkaline into the cotton, not only a safe operation but also a precise control of the discharge capacity can be obtained, leading to a very practical power source for miniwatt applications. Moreover, the Al self-corrosion is also

inhibited successfully due to the impeded OH$^-$ diffusion inside cotton. The cotton-based Al-air battery system can achieve a very high peak power density of 73 mW cm^{-2}, which is about one order of magnitude higher than other paper-based energy devices in literature. A high specific capacity of 940 mA h g^{-1} and a high specific energy of 930 mW h g^{-1} were also obtained at 10 mA cm^{-2}, surpassing the existing Li ion batteries. As for its voltage output, it can be conveniently improved by developing multi-cell battery pack, of which a two-cell battery pack with 2.7 V OCV and 223.8 mW power output was demonstrated. This low-cost and renewable battery technology is especially suitable for recharging various miniwatt electronics in the outdoor environment, where the grid is not accessible and the energy density is of key importance.

Declaration of competing interest

The authors declare that they have no known competing financial interests or personal relationships that could have appeared to influence the work reported in this paper.

Acknowledgement

Appendix A. Supplementary data

Supplementary data to this article can be found online at https://doi.org/10.1016/j.gee.2021.05.003.

References

[1] R. O'hayre, S.-W. Cha, W. Colella, F.B. Prinz, Fuel Cell Fundamentals, John Wiley & Sons, 2016.

[2] F. Cheng, J. Chen, Chem. Soc. Rev. 41 (2012) 2172−2192.

[3] A. Kraytsberg, Y. Ein-Eli, J. Power Sources 196 (2011) 886−893.

[4] P. Gu, M. Zheng, Q. Zhao, X. Xiao, H. Xue, H. Pang, J. Mater. Chem. 5 (2017) 7651−7666.

[5] Y. Liu, Q. Sun, W. Li, K.R. Adair, J. Li, X. Sun, Green Energy Environ. 2 (2017) 246−277.

[6] T. Zhang, Z. Tao, J. Chen, Mater. Horiz. 1 (2014) 196−206.

[7] D. Egan, C.P. De León, R. Wood, R. Jones, K. Stokes, F. Walsh, J. Power Sources 236 (2013) 293−310.

[8] M. Mokhtar, M.Z.M. Talib, E.H. Majlan, S.M. Tasirin, W.M.F.W. Ramli, W.R.W. Daud, J. Sahari, J. Ind. Eng. Chem. 32 (2015) 1−20.

[9] E. Shkolnikov, A. Zhuk, M. Vlaskin, Renew. Sustain. Energy Rev. 15 (2011) 4611−4623.

[10] S. Zaromb, J. Electrochem. Soc. 109 (1962) 1125−1130.

[11] R. Mori, Electrochem. Energy Rev. 3 (2020) 344−369.

[12] L. Fan, H. Lu, J. Leng, Electrochim. Acta 165 (2015) 22−28.

[13] J. Ma, J. Wen, J. Gao, Q. Li, Electrochim. Acta 129 (2014) 69−75.

[14] I.-J. Park, S.-R. Choi, J.-G. Kim, J. Power Sources 357 (2017) 47−55.

[15] Y. Xue, S. Sun, Q. Wang, H. Miao, S. Li, Z. Liu, Electrochim. Acta 230 (2017) 418−427.

[16] M. Li, J. Yuan, B. Nan, Y. Zhu, S. Yu, Y. Shi, M. Yang, Z. Wang, Y. Gu, Z. Lu, Electrochim. Acta 249 (2017) 413−420.

[17] K. Liu, Z. Zhou, H.-Y. Wang, X. Huang, J. Xu, Y.-G. Tang, J. Li, H. Chu, J. Chen, RSC Adv. (2016).

[18] M. Deyab, Electrochim. Acta 244 (2017) 178−183.

[19] D. Wang, D. Zhang, K. Lee, L. Gao, J. Power Sources 297 (2015) 464−471.

[20] E. Grishina, D. Gelman, S. Belopukhov, D. Starosvetsky, A. Groysman, Y. Ein-Eli, ChemSusChem 9 (2016) 2103−2111.

[21] S. Yang, H. Knickle, J. Power Sources 112 (2002) 162−173.

[22] Y. Liu, Q. Sun, X. Yang, J. Liang, B. Wang, A. Koo, R. Li, J. Li, X. Sun, ACS Appl. Mater. Interfaces 10 (2018) 19730−19738.

[23] A. Mohamad, Corrosion Sci. 50 (2008) 3475−3479.

[24] G. Wu, S. Lin, C. Yang, J. Membr. Sci. 280 (2006) 802−808.

[25] Y. Xu, Y. Zhao, J. Ren, Y. Zhang, H. Peng, Angew. Chem. Int. Ed. 55 (2016) 7979−7982.

[26] Y. Wang, W. Pan, H.Y. Kwok, H. Zhang, X. Lu, D.Y. Leung, J. Power Sources 437 (2019) 226896.

[27] A. Avoundjian, V. Galvan, F.A. Gomez, Micromachines 8 (2017) 222.

[28] L.-L. Shen, G.-R. Zhang, M. Biesalski, B.J. Etzold, Lab Chip 19 (2019) 3438−3447.

[29] Y. Wang, H. Kwok, W. Pan, H. Zhang, D.Y. Leung, J. Power Sources 414 (2019) 278−282.

[30] Y. Wang, H.Y. Kwok, W. Pan, H. Zhang, X. Lu, D.Y. Leung, Appl. Energy 251 (2019) 113342.

[31] Y. Wang, H.Y. Kwok, W. Pan, Y. Zhang, H. Zhang, X. Lu, D.Y. Leung, Electrochim. Acta 319 (2019) 947−957.

[32] Y. Wang, H.Y. Kwok, W. Pan, Y. Zhang, H. Zhang, X. Lu, D.Y. Leung, J. Power Sources 450 (2020) 227685.

[33] Y.-J. Cho, I.-J. Park, H.-J. Lee, J.-G. Kim, J. Power Sources 277 (2015) 370−378.

[34] J. Ren, C. Fu, Q. Dong, M. Jiang, A. Dong, G. Zhu, J. Zhang, B. Sun, ACS Sustain. Chem. Eng. 9 (2021) 2300−2308.

[35] C.-C. Yang, S.-S. Chiu, S.-C. Kuo, T.-H. Liou, J. Power Sources 199 (2012) 37−45.

[36] J. Li, Z. Zhou, K. Liu, F. Li, Z. Peng, Y. Tang, H. Wang, J. Power Sources 343 (2017) 30−38.

[37] Y. Xue, H. Miao, S. Sun, Q. Wang, S. Li, Z. Liu, J. Power Sources 342 (2017) 192−201.

[38] B.J. Hopkins, Y. Shao-Horn, D.P. Hart, Science 362 (2018) 658−661.

[39] G.M. Dorris, D.G. Gray, J. Chem. Soc., Faraday Trans. 1 77 (1981) 713−724.

[40] S.C. Fernandes, J.A. Walz, D.J. Wilson, J.C. Brooks, C.R. Mace, Beyond Wicking: Expanding the Role of Patterned Paper as the Foundation for an Analytical Platform, ACS Publications, 2017.

[41] J. Xuan, D. Leung, H. Wang, M.K. Leung, B. Wang, M. Ni, Appl. Energy 104 (2013) 400−407.